Engineered Science
DOI: https://dx.doi.org/10.30919/es8d822

The Effects of Fe Addition for Enhanced Thermoelectric Performance in p-type $CuAlO_2$

Yining Feng[1], Jin Hong Joo[2], Guangshuai Han[1] and Na Lu[1, 3,*]

Abstract

Defect engineering is an effective method to enhance the power factor of a thermoelectric material by modulating its band structure. For cuprous delafossite oxides, the limitations in achieving an outstanding figure of merit [zT] are due to their intrinsically low charge carrier mobility and high thermal conductivity. Herein, we apply defect engineering via doping $CuAl_{1-x}Fe_xO_2$ with x=0.05, 0.1, 0.2 at different deposition temperatures to overcome the aforementioned issues. The effects of Fe doping on both electronic properties and thermal conductivity have been systematically studied. The addition of Fe was found to enhance the electrical conductivity with an increased carrier density. The mass difference between Al and Fe resulted in phonon scattering, which significantly reduced the thermal conductivity. As a result, the ultra-low thermal conductivity of 0.776 W/m·K was obtained at 773 K for $CuAl_{0.8}Fe_{0.2}O_2$. Detailed analyses of the temperature-dependent Seebeck coefficient, electrical conductivity, and thermal conductivity with materials properties have been discussed. The effect of Fe addition is advantageous for the improvement of $CuAlO_2$ thermoelectric properties.

Keywords: Thermoelectric; Fe doping; Delafossite oxides; Low lattice thermal conductivity.
Received: 02 December 2022; Revised: 08 February 2023; Accepted: 19 February 2023.
Article type: Research article.

1. Introduction

Thermoelectric (TE) technology has gained popularity as a potential renewable energy source to replace conventional ones. Due to the issues including, but not limited to, environmental impacts, political controversies, and shortage concerns, energy generation can no longer rely upon conventional energy sources such as fossil fuels.[1] The use of TE technology can relieve some of the aforementioned issues. However, the broader application of TE is hindered by materials toxicity, high cost, thermal stability, and moderate conversion of energy.[2] To improve the limitations, studies have been conducted to explore various promising oxides TE materials and their properties.[3–6] Cuprous delafossite oxides $CuMO_2$ (M=Al, Cr, Fe, Mn, *etc*) transport properties in optoelectronics devices have been widely studied. However, its application in the thermoelectric area has not been fully explored. Due to the localized oxygen p-type nature of the valence band, $CuAlO_2$ has low mobility and high thermal conductivity were major factors that impeded the realization of a high zT.[7,8]

The efficiency of a TE material is determined by the figure of merit (zT) which includes both electrical and thermal properties. It can be written in the dimensionless form of

$$zT = \frac{S^2\sigma}{k_T}T \quad (1)$$

where S is the Seebeck coefficient, σ is the electrical conductivity, k_T is the total thermal conductivity, and T is the absolute temperature. Due to the interdependence of three parameters, there is a trade-off between power factor and thermal conductivity to reach an optimized zT.

Defect engineering is one of the effective approaches for improving the TE efficiency of $CuAlO_2$ alloys by enhancing their electronic properties or reducing lattice thermal conductivity via additions of the dopants.[9–12] Several studies have investigated using different dopants to further enhance the electronic properties of $CuAlO_2$ alloys. Sakulkalavek *et al.*

[1] *Lyles School of Civil Engineering, Sustainable Materials, and Renewable Technology (SMART) Lab, Purdue University, West Lafayette, IN 47906, U.S.A.*
[2] *Davidson School of Chemical Engineering, Purdue University, West Lafayette, IN 47906, U.S.A.*
[3] *School of Materials Engineering, Birck Nanotechnology Center, Purdue University, West Lafayette, IN 47906, U.S.A.*
**Email:* luna@purdue.edu (N. Lu)

reported an enhancement in the electrical conductivity of p-type $CuAlO_2$ by Ag_2O addition caused by the increased carrier density.[13] As the interdependence of electrical and thermal conductivity, high electrical conductivity will lead to an increase in thermal conductivity. However, a large value of thermal conductivity limited the broader application of thermoelectric. The Ca substitution in $CuAl_{1-x}Ca_xO_2$ up to x=0.1 showed an increased power factor contributes by both electrical conductivity and the Seebeck coefficient.[14] The lack of a thermal conductivity study remains an uncertainty to conclude the effectiveness of using Ca dopant. Another study on Cr substitution has been predicted to increase the density of states at the top of the valence band through DFT simulations, which showed the promise of electronic properties improvement.[15] Co-doping of two different substituents was also investigated to further increase the electrical conductivity. It was found that the power factor was substantially improved by the addition of both Ag and Zn which reaches a value of 1.26×10^{-4} $Wm^{-1}K^{-2}$ 1060 K.[16] The result is similar to the study on the effects of Fe addition. Park *et al*. reported that Fe addition up to x = 0.1 significantly increased the power factor because of a significant increase in electrical conductivity. The highest value measured was 1.1×10^{-4} $W/m{\cdot}K^2$ for x = 0.1 at 1140 K.[17] Also, several other studies on Fe doping showed the feasibility of the enhancement of the power factor caused by increased carrier density.[18–20] To the best of our knowledge, there has been no report on the phonon transport effects on zT of $CuAlO_2$ by the addition of point defects.

Herein, this paper aims to enhance the thermoelectric properties of $CuAlO_2$ by incorporating Fe_2O_3. Due to the mass difference between Fe and Al (M_{Fe}=55.845u, M_{Al}=26.98u), we anticipated the substitution of Fe to scatter phonons effectively. As a result, the multiscale defects (point defects, grain boundaries) significantly reduce the lattice thermal conductivity to ~0.776 W/m·K at 773 K, which is the lowest reported lattice thermal conductivity at high temperature for $CuAl_{1-x}Fe_xO_2$.

2. Experimental

2.1 Sample preparation

Fe-doped samples of $CuAl_{1-x}Fe_xO_2$ (x=0.05, 0.1, and 0.2) were stoichiometrically mixed using Al_2O_3, CuO, and Fe_2O_3 powder with alcohol using the solid-state method by ball milling. The ball milled blurry was dried at 100˚C overnight and then annealed at different temperatures and duration in air. The resultant powders were cold pressed into pellets with 13mm diameter and 2mm thickness.

2.2 Sample characterization

The phase composition of as-annealed powders was analyzed via powder X-ray diffraction (XRD; Panalytical Empyrean) using Cu Kα radiation with Bragg-Brentano mode at 40 kV and 40 mA. The microstructure of as-annealed powders was investigated by a scanning electron microscope (SEM; FEI Nova NanoSEM). The elements dispersion of the $CuAl_{0.9}Fe_{0.1}O_2$ sample was observed by energy dispersive X-ray spectrometer (EDS).

The details of the temperature-dependent Seebeck coefficient were determined through a home-built measurement system in a vacuum chamber as described in our previous publications.[7,21] The S was calculated from the slope of temperature vs voltage. Temperature-dependent electrical conductivity was directly measured by the hall effect using the Van der Pauw method (Ecopia AHT55T5). The thermal conductivity was calculated via $\kappa = \rho C_p D$, where C_p is the measured specific heat and D is the measured thermal diffusivity by laser flash method (LFA 467, NETZSCH, Germany) using the transient time-dominant method. All the TE properties were measured from 300 K to 780 K in a nitrogen environment. The uncertainty of each measured transport property is about 5%.

3. Results and discussion

The experiments on different annealing temperatures and times have been conducted to determine the optimized growth conditions for $CuAl_{1-x}Fe_xO_2$ samples. The crystallinity of as-annealed $CuAl_{0.9}Fe_{0.1}O_2$ powders is investigated by XRD. All the samples are polycrystalline as patterns shown in Fig. 1 (a). The main peaks in samples could be indexed to the rhombohedral phase (Space group of $R\bar{3}m$). The measured lattice parameters are in good agreement with the computational results for this material[17] Monoclinic baddeleyite (ZrO_2) is detected as a unique zirconia phase in all composite samples, in accordance with the phase diagrams. Annealing at 1060 °C for 12 hours leads to the raw materials are not fully reacted, on the other hand, annealing at 1150°C for 20 hours results in a second phase in the samples, as shown in Fig. 1(a) back and blue line, respectively. The high phase purity of the sample is obtained by annealing the materials at 1060°C for 20 hours in the air, as shown in the red line, Fig. 1(a).

The different Fe-doped $CuAl_{1-x}Fe_xO_2$ powders have been synthesized following the stoichiometric equation as shown below. The powders with different Fe doping concentrations have been annealed at 1060 °C for 20h in the air for enhanced phase purity. The results in XRD patterns are shown in Fig. 1(b). All the main peaks agree well with the rhombohedral

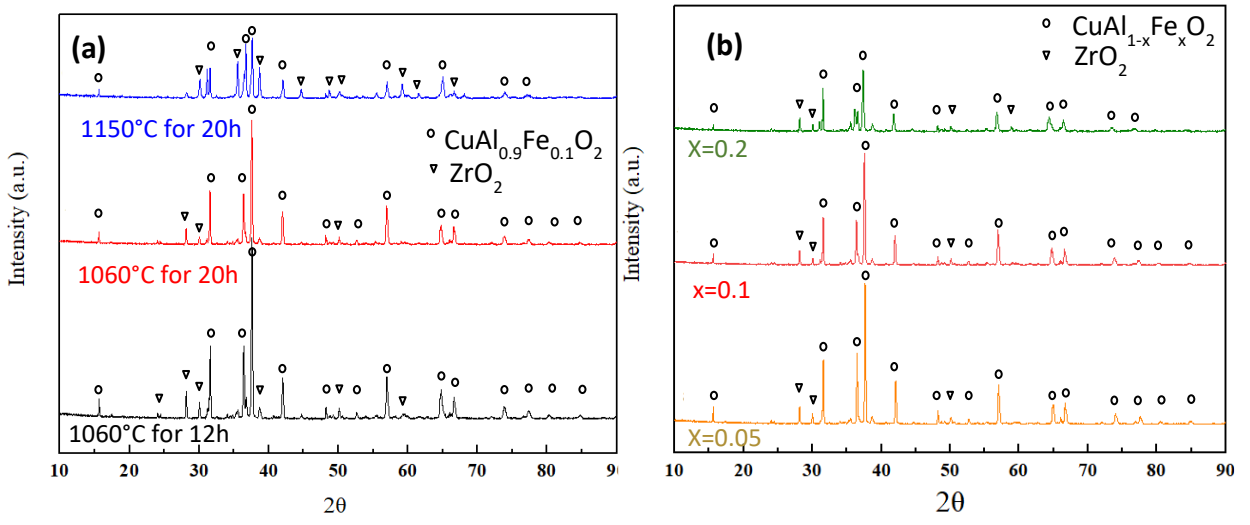

Fig. 1 XRD patterns of phase composition and crystal structure study for $CuAl_{1-x}Fe_xO_2$ powders. (a) $CuAl_{1-x}Fe_xO_2$ under different annealing temperature and time; (b) stoichiometric $CuAl_{1-x}Fe_xO_2$ powders annealed under 1060°C for 20h in air.

structure that indicated high phase purity. The width of XRD peaks decreases with the increase of Fe doping concentrations. This is due to the grain size growing with the addition of Fe_2O_3. The optimized Fe doping concentration will be determined by measuring the material's thermoelectric properties.

$$CuO + \frac{1-x}{2}Al_2O_3 + \frac{x}{2}Fe_2O_3 \rightarrow CuAl_{1-x}Fe_xO_2 + \frac{1}{4}O_2$$

Figure 2 shows SEM micrographs of powder sample $CuAl_{1-x}Fe_xO_2$. The grain size increases from 0.8 μm to 2.5 μm as the amount of Fe in the $CuAl_{1-x}Fe_xO_2$ samples increases. When x=0.2, the grain size is much larger compared to others as shown in Fig. 2(c), which agrees with the XRD results discussed above. There are a few small particles attached on the surface of $CuAl_{1-x}Fe_xO_2$ powders that are ZrO_2 residuals during the ball milling process as observed in SEM images. It is also observed ZrO_2 peak in XRD results. The phase composition of annealed $CuAl_{0.9}Fe_{0.1}O_2$ powder was analyzed by SEM/EDS, as shown in Fig. 2(d). The element mapping of

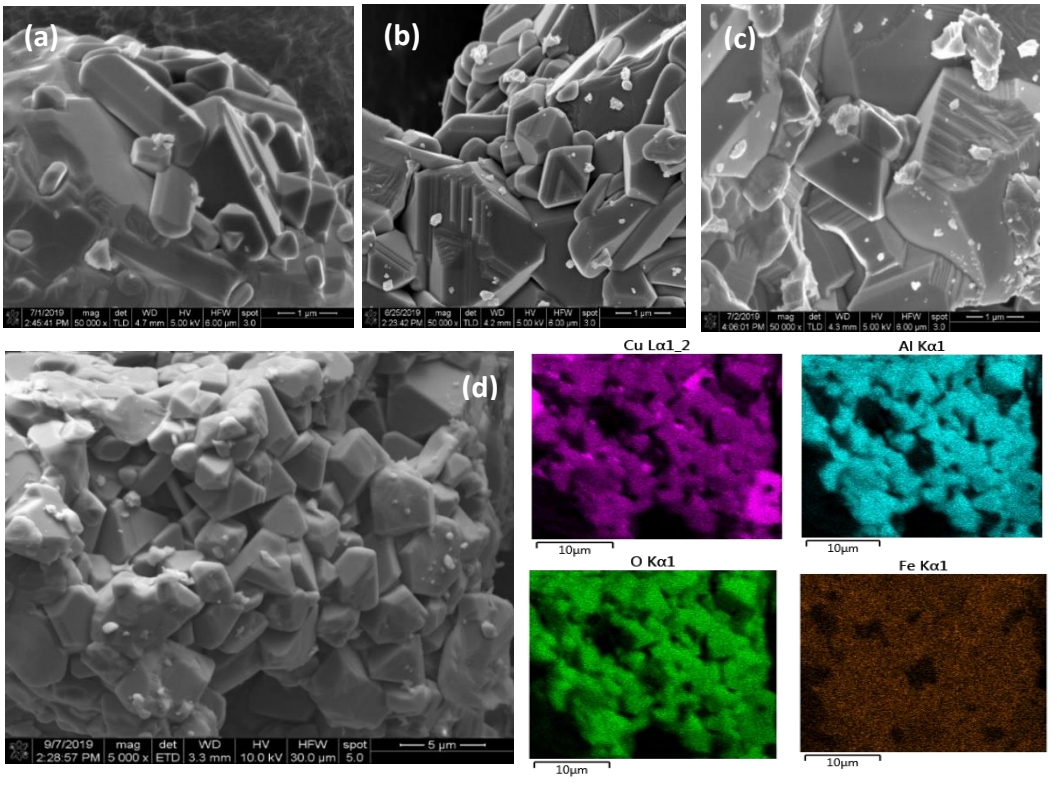

Fig. 2 SEM micrographs of stoichiometric $CuAl_{1-x}Fe_xO_2$ powders annealed under 1060 °C for 20h in air (a) $CuAl_{0.95}Fe_{0.05}O_2$; (b) $CuAl_{0.9}Fe_{0.1}O_2$; (c) $CuAl_{0.8}Fe_{0.2}O_2$; (d) EDS element maps for as-annealed $CuAl_{0.9}Fe_{0.1}O_2$ powder.

the sample shows uniformly distributed in the annealed powders, presenting high phase purity of the samples. The atomic ratio for Cu: Al: O is 1:1:4.

The electronic transport properties of pressed pellets have been conducted by Hall measurement using the four-point probe method. Temperature-dependent electrical conductivity and mobility results of $CuAlO_2$ with different Fe doping concentrations are shown in Fig. 3(a). Overall, electrical conductivity increases with the increase in temperature showing semiconductor behavior. With the increasing temperature thermal energy excites more free electrons hopping from the valence band to the conduction band resulting in enhanced electrical conductivity. Compared to the electrical conductivity of undoped $CuAlO_2$ is about 17 S/m at 780 K,[7] Fe doping $CuAlO_2$ shows a nearly three times higher value of ~45 S/m at the same temperature. The addition of Fe dopant effectively increases free holes that enhance the carrier concentration, which contributes to higher electrical conductivity. It is notable to see that Fe doping composition at 0.1 is the optimized doping concentration that reaches high electrical conductivity over the temperature. This may due to the higher value of mobility as shown in Fig. 3(b). The relationship between electrical conductivity and mobility is shown below:

$$\sigma = qn\mu \tag{2}$$

where μ is the mobility, n is the carrier concentration, and q is the charge per electric charge.

With the addition of Fe up to x=0.1, the increase of the density makes a more significant contribution to the reduction of the scattering process that enhances the mobility. To understand the different scattering mechanisms, the scattering factor can be obtained from the relationship between hall mobility and temperature, as shown below:

$$\mu \propto T^{-\frac{3}{2}+r} \tag{3}$$

where μ is the hall mobility, T is temperature, and r is the scattering factor.

In Fig. 3(b), temperature-dependent mobility for $CuAl_{1-x}Fe_xO_2$ shows a rough trend of $\mu \sim T^{-1.5}$ over the entire temperature range. This indicates that acoustic deformation potential scattering (ADP) with r= 0 has dominated the scattering mechanism. This result can also be confirmed by Fig. 1, where the FeO-$CuAlO_2$ alloy exists in the sample. However, the electrical conductivity of $CuAl_{0.8}Fe_{0.2}O_2$ is lower. This is because Fe_2O_3 has low electrical conductivity. If the addition of Fe content is greater than 0.2, the overall electrical conductivity will decrease due to low mobility.

Due to the interdependent nature of all TE parameters (S, σ, k), high electrical conductivity does not guarantee better TE performance as the Seebeck coefficient may deteriorate. Fig. 4 shows the temperature-dependent Seebeck coefficient of $CuAl_{1-x}Fe_xO_2$ (x=0, 0.05, 0.1, and 0.2). The sign of the Seebeck coefficient is positive, indicating the majority of carriers are holes and present p-type behavior. The Seebeck coefficient values of $CuAl_{0.9}Fe_{0.1}O_2$ and $CuAl_{0.8}Fe_{0.2}O_2$ increases with the increasing temperature and then decrease. Compared to the undoped $CuAlO_2$ Seebeck coefficient value, the Fe addition up to 0.1 decreases the Seebeck coefficient as the maximum value of 600 μV/K at 500K. This implies that the addition of Fe leads to an increase in carrier concentration. The inverse relationship between the Seebeck coefficient and carrier concentration:

$$S = \left(\frac{8\pi^2 k^2 B}{3eh^2}\right) m^* T \left(\frac{\pi}{3n}\right)^{2/3} \tag{4}$$

where m^* is the density of state effective mass and n is the carrier concentration.

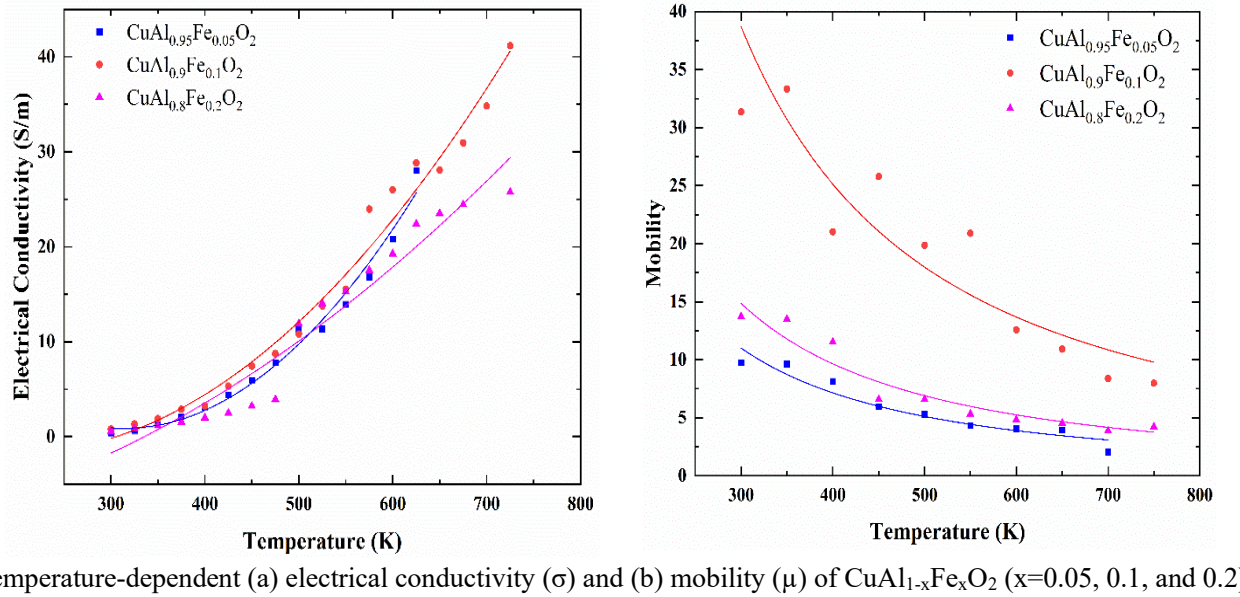

Fig. 3 Temperature-dependent (a) electrical conductivity (σ) and (b) mobility (μ) of $CuAl_{1-x}Fe_xO_2$ (x=0.05, 0.1, and 0.2).

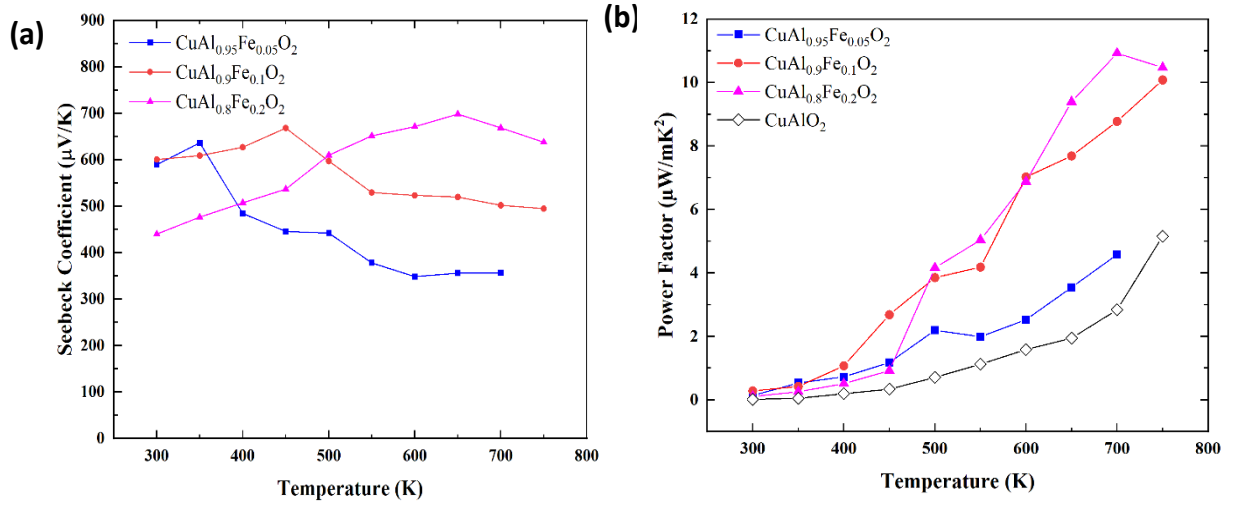

Fig. 4 Temperature dependent (a) Seebeck coefficient (*S*) and (b) power factor (PF) of $CuAl_{1-x}Fe_xO_2$ (x=0, 0.05, 0.1, and 0.2).

The increasing carrier concentration by doping Fe enhances the electrical conductivity but simultaneously deteriorates the Seebeck coefficient. The power factor is found to increase with increasing temperature, as shown in Fig. 4(b). For power generation applications where the heat source is unlimited, the PF of the TE materials may be a more important parameter than the zT. $CuAl_{0.8}Fe_{0.2}O_2$ shows the highest PF value of 11 $\mu W/mK^2$ at 700K, which is two orders of magnitude higher than the reported $CuAlFeO_2$ in the previous study.[7] Adding Fe dopants increases electrical conductivity without degrading the Seebeck coefficient too much which contributes to the high PF of $CuAl_{0.8}Fe_{0.2}O_2$. High purity of the samples and annealing process as we discussed above are critical steps to ensure the high electrical performance of the TE materials.

One of the strategies to enhance the efficiency of TE materials is to minimize thermal conductivity. Total thermal conductivity (k_T) consists of the contributions from both electron and phonon transport, defined as follows:

$$k_T = k_e + k_l \quad (5)$$

where electronic contribution can be approximately estimated by $k_e = L\sigma T = nq\mu LT$, L is the Lorenz factor (2.45×10^{-8} J^2 K^{-2} C^{-2}), and lattice contribution k_l. Owing to a low k_e based on a previous study, k_T largely comes from the lattice contributions for bulk semiconductor materials.[21]

Temperature-dependent lattice thermal conductivity of $CuAl_{1-x}Fe_xO_2$ (x=0.05, 0.1, and 0.2) is shown in Fig. 5(a). For different Fe concentrations, samples show a similar trend in temperature-dependent thermal conductivity. At low temperatures, the thermal conductivity increases due to the group velocity enhancement caused by lattice vibrations. At higher temperatures, more scattering occurs as phonon-phonon Umklapp scattering may dominate the process. It shows the decreasing trend of thermal conductivity. With the

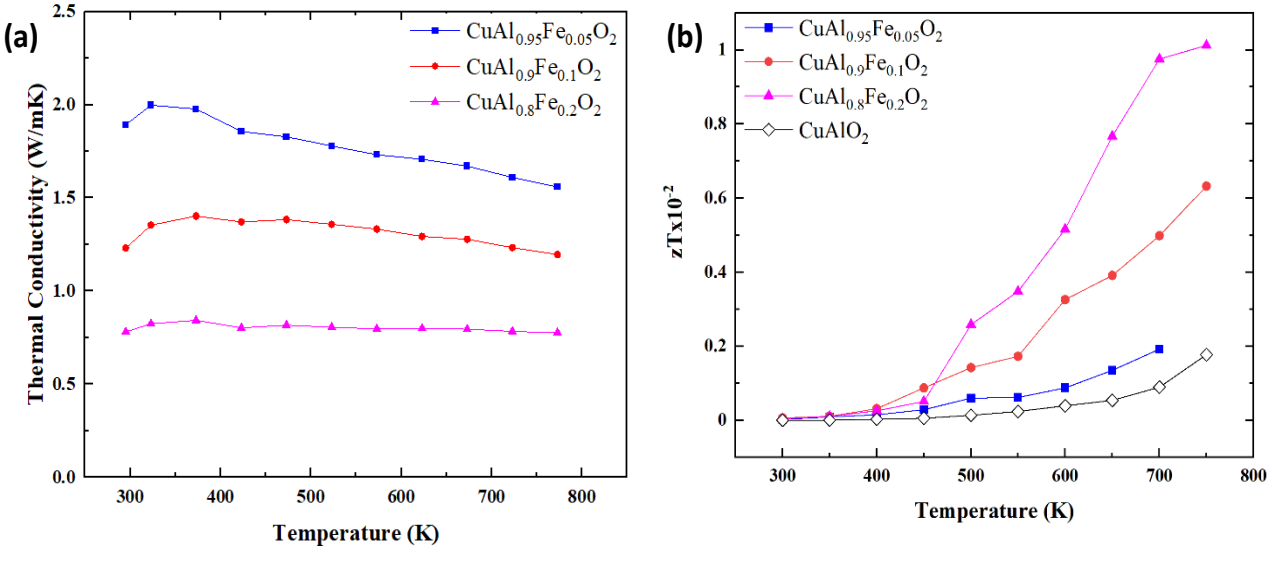

Fig. 5 Temperature dependent (a) thermal conductivity (*k*) and (b) figure of merit (zT) of $CuAl_{1-x}Fe_xO_2$ (x=0, 0.05, 0.1, and 0.2).

Fe incorporation increasing, lattice thermal conductivity reduces over the entire temperature range. As the mass difference exists between Al and Fe, the phonon scattering can be intensified by the alloys and defects. Based on SEM results, $CuAl_{0.8}Fe_{0.2}O_2$ nanoparticles exhibit more grain boundary that limits the phonon mean free path, which enhances the phonon scattering compared to other samples. Thus, $CuAl_{0.8}Fe_{0.2}O_2$ presents the lowest thermal conductivity ~0.776W/mK at 773K. This value is much lower than conventional thermoelectric material such as BiSbTe.[22] This ultra-low thermal conductivity shows the feasibility of $CuAl_{0.8}Fe_{0.2}O_2$ used as p-type thermoelectric material.

The zT values for $CuAl_{1-x}Fe_xO_2$ (x=0, 0.05, 0.1, and 0.2) are shown in Fig. 5(b). It is found that zT increases with the temperature increasing. Because Fe doping can enhance the power factor and lower the thermal conductivity of $CuAlO_2$, the sample $CuAl_{0.8}Fe_{0.2}O_2$ has the maximum zT value of 1.2×10^{-2} at 750K. This value is one order magnitude improvement than that of undoped $CuAlO_2$ reported previously.[7] Further strategies for the zT enhancement: (1) using a simulation tool to predict the optimized doping concentration for $CuAl_{1-x}Fe_xO_2$ as guidance for experiments. The predicted power factor can be used as a baseline to compare; (2) further control the nanostructure of the sample to ensure the thermal conductivity will remain as low as possible. Thus, higher zT will be reached by optimizing carrier concentration with a high power factor and low thermal conductivity.

4. Conclusions

In summary, Fe-doped $CuAlO_2$ nanoparticles have been successfully synthesized by the solid-state method. The addition of Fe_2O_3 nanoparticles resulted in the enhancement of zT for $CuAlO_2$ by defect engineering. Measurements reveal that the carrier concentration is at an optimized level while the mobility increases through the addition of Fe_2O_3 up to 10%, which directly improves the electrical properties with the peak power factor of 11 $\mu W/mK^2$ at 700K. Moreover, the addition of Fe_2O_3 results in enhanced phonon scattering, which promotes the reduction of lattice thermal conductivity from 1.7 W/mK to 0.776 W/mK at 773K. Therefore, the result in TE performance is significantly enhanced with the peak zT value of 1.2×10^{-2} at 750K, about one order magnitude improvement than that of undoped $CuAlO_2$. The p-type behavior and enhanced TE properties of $CuAlO_2$ open up more opportunities using cuprous delafossite oxides in thermoelectric and beyond.

Acknowledgment

The authors at Purdue University are grateful for the financial support from the National Science Foundation CAREER program (under Grants of CMMI – 1560834) and NSF PFI-TT 1919191.

Conflict of Interest

There is no conflict of interest.

Supporting Information

Not applicable.

References

[1] T. M. Tritt, Thermoelectric phenomena, materials, and applications, *Annual Review of Materials Research*, 2011, **41**, 433-448, doi: 10.1146/annurev-matsci-062910-100453.

[2] N. Lu, I. Ferguson, III-nitrides for energy production: Photovoltaic and thermoelectric applications, *Semiconductor Science and Technology*, 2013, **28**, 1–11, doi: 10.1088/0268-1242/28/7/074023.

[3] Y. Feng, X. Jiang, E. Ghafari, B. Kucukgok, C. Zhang, I. Ferguson, N. Lu, Metal oxides for thermoelectric power generation and beyond, *Advanced Composites and Hybrid Materials*, 2018, **1**, 114-126, doi: 10.1007/s42114-017-0011-4.

[4] N. Lu, C. Zhou, Y. Wang, A.M. Elquist, A. Ghods, I.T. Ferguson, V.G. Saravade, A review of earth abundant ZnO-based materials for thermoelectric and photovoltaic applications, in: F.H. Teherani, D.C. Look, D.J. Rogers (Eds.), Oxide-Based Materials and Devices IX, SPIE, 2018, 53, doi: 10.1117/12.2302467.

[5] C. Zhou, A. Ghods, V. G. Saravade, P. V Patel, K.L. Yunghans, C. Ferguson, Y. Feng, B. Kucukgok, N. Lu, I.T. Ferguson, Review-The Current and Emerging Applications of the III-Nitrides, *ECS Journal of Solid-State Science and Technology*, 2017, **6**, 149-156, doi: 10.1149/2.

[6] B. Kucukgok, B. Hussain, C. Zhou, I. T. Ferguson, N. Lu, Thermoelectric properties of ZnO thin films grown by metal-organic chemical vapor deposition, *MRS Online Proceedings Library*, 2015, **1805**, 1-6, doi: 10.1557/opl.2015.687.

[7] Y. Feng, A. Elquist, Y. Zhang, K. Gao, I. Ferguson, A. Tzempelikos, N. Lu, Temperature dependent thermoelectric properties of cuprous delafossite oxides, *Composites Part B: Engineering*, 2019, **156**, 108-112, doi: 10.1016/j.compositesb.2018.08.070.

[8] E. Witkoske, D. Guzman, Y. Feng, A. Strachan, M. Lundstrom, N. Lu, The use of strain to tailor electronic thermoelectric transport properties: a first principles study of 2H-phase $CuAlO_2$, *Journal of Applied Physics*, 2019, **125**, 082531, doi: 10.1063/1.5058275.

[9] E. Witkoske, Z. Tong, Y. Feng, X. Ruan, M. Lundstrom, N. Lu, The use of strain and grain boundaries to tailor phonon transport properties: A first-principles study of 2H-phase $CuAlO_2$ II, *Journal of Applied Physics*, 2020, **127**, 115108, doi:

10.1063/1.5142485.
[10] N. Daichakomphu, R. Sakdanuphab, A. Harnwunggmoung, Y. Puarporn, N. Chanlek, A. Sakulkalavek, Enhanced carrier concentration of Fe doped delafossite $CuAlO_2$ by double-effect: Divalent metal ions doping and excess oxygen, *Solid State Ionics*, 2018, **328**, 17-24, doi: 10.1016/j.ssi.2018.11.007.
[11] H. Wang, A. D. LaLonde, Y. Pei, G. J. Snyder, The criteria for beneficial disorder in thermoelectric solid solutions, *Advanced Functional Materials*, 2013, **23**, 1586-1596, doi: 10.1002/adfm.201201576.
[12] Z. Liu, B. Fu, X. Yi, G. Yuan, J. Wang, J. Li, L. Luna, I. Ferguson, Co-doping of magnesium with indium in nitrides: first principle calculation and experiment, *RSC Advances*, 2016, **6**, 5111-5115, doi: 10.1039/c5ra24642c.
[13] P. Sarayut, Enhancing the electrical conductivity and thermoelectric figure of merit of the p-type delafossite $CuAlO_2$ by Ag_2O addition, *Current Applied Physics*, 2017, **17**, 1264-1270, doi: 10.1016/j.cap.2017.06.011.
[14] K. Park, K. Y. Ko, W.-S. Seo, Effect of partial substitution of Ca for Al on the microstructure and high-temperature thermoelectric properties of $CuAlO_2$, *Materials Science and Engineering: B*, 2006, **129**, 1-7, doi: 10.1016/j.mseb.2005.10.035.
[15] D. O. Scanlon, A. Walsh, B. J. Morgan, G. W. Watson, D. J. Payne, R. G. Egdell, Effect of Cr substitution on the electronic structure of $CuAl_{1-x}Cr_xO_2$, *Physical Review B*, 2009, **79**, 035101, doi: 10.1103/physrevb.79.035101.
[16] S.-I. Yanagiya, N. Van Nong, J. Xu, N. Pryds, The effect of (Ag, Ni, Zn)-addition on the thermoelectric properties of copper aluminate, *Materials*, 2010, **3**, 318-328, doi: 10.3390/ma3010318.
[17] K, Park, Improvement in thermoelectric properties of $CuAlO_2$ by adding Fe_2O_3, *Journal of Alloys and Compounds*, 2007, **437**, 1-6, doi: 10.1016/j.jallcom.2006.07.067.
[18] Yi-Cheng, Liou, Effects of mechanical milling on preparation and properties of $CuAl_{1-x}Fe_xO_2$ thermoelectric ceramics, *Ceramics International*, 2012, **38**, 3619-3624, doi: 10.1016/j.ceramint.2011.12.079.
[19] D. Huang, J. Lin, M. J. Nilges, Y. Pan, Local structures and roles of Fe_{3+} and Cr_{3+} in p-type semiconductor $CuAlO_2$, *Physica Status Solidi (b)*, 2012, 249, 1559-1565, doi: 10.1002/pssb.201147466.
[20] V. Siriwongrungson, A. Sakulkalavek, R. Sakdanuphab, Optimum sintering temperature for thermoelectric properties of low-cost CuAl0.90Fe0.10O2 material, *Journal of Materials Science: Materials in Electronics*, 2016, **27**, 11102-11109, doi: 10.1007/s10854-016-5227-5.
[21] E. N. Hurwitz, M. Asghar, A. Melton, B. Kucukgok, L. Su, M. Orocz, M. Jamil, N. Lu, I. T. Ferguson, Thermopower study of GaN-based materials for next-generation thermoelectric devices and applications, *Journal of Electronic Materials*, 2011, **40**, 513-517, doi: 10.1007/s11664-010-1416-9.
[22] B. Poudel, Q. Hao, Y. Ma, Y. Lan, A. Minnich, B. Yu, X. Yan, D. Wang, A. Muto, D. Vashaee, X. Chen, J. Liu, M. S. Dresselhaus, G. Chen, Z. Ren, High-thermoelectric performance of nanostructured bismuth antimony telluride bulk alloys, *Science*, 2008, **320**, 634-638, doi: 10.1126/science.1156446.